Cell Reports

Report

Loss of Muscle MTCH2 Increases Whole-Body Energy Utilization and Protects from Diet-Induced Obesity

Graphical Abstract

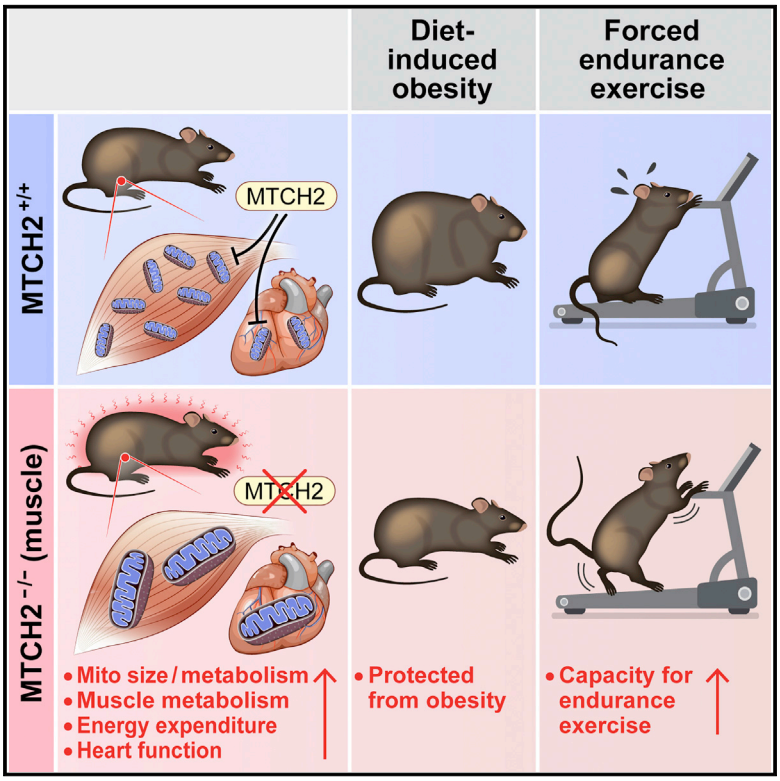

Highlights

- MTCH2 acts as a repressor of muscle mitochondrial metabolism and size
- Loss of MTCH2 increases muscle metabolism, energy expenditure, and heart function
- Mice deficient in muscle MTCH2 demonstrate an increased capacity for endurance exercise
- Mice deficient in muscle MTCH2 are protected from diet-induced obesity

Authors

Liat Buzaglo-Azriel, Yael Kuperman, Michael Tsoory, ..., Michal Haran, Cecile Vernochet, Atan Gross

Correspondence

atan.gross@weizmann.ac.il

In Brief

The MTCH2 locus is associated with increased obesity in humans. Buzaglo-Azriel et al. show that muscle MTCH2 deficiency in mice provides protection from a high-fat diet and that this protection is most likely due to increased muscle metabolism, leading to elevated whole-body energy demand and heat production.

Buzaglo-Azriel et al., 2016, Cell Reports *14*, 1602–1610
February 23, 2016
http://dx.doi.org/10.1016/j.celrep.2016.01.046

CellPress

OPEN ACCESS
CellPress

Cell Reports
Report

Loss of Muscle MTCH2 Increases Whole-Body Energy Utilization and Protects from Diet-Induced Obesity

Liat Buzaglo-Azriel,[1] Yael Kuperman,[2] Michael Tsoory,[2] Yehudit Zaltsman,[1] Liat Shachnai,[1] Smadar Levin Zaidman,[3] Elad Bassat,[1] Inbal Michailovici,[1] Alona Sarver,[1] Eldad Tzahor,[1] Michal Haran,[4] Cecile Vernochet,[5] and Atan Gross[1,*]
[1]Department of Biological Regulation, Weizmann Institute of Science, Rehovot 76100, Israel
[2]Department of Veterinary Resources, Weizmann Institute of Science, Rehovot 76100, Israel
[3]Department of Chemical Research Support, Weizmann Institute of Science, Rehovot 76100, Israel
[4]Hematology Institute, Kaplan Medical Center, Rehovot 76100, Israel
[5]Cardiovascular, Metabolic, and Endocrine Diseases (CVMED) Research Unit, Pfizer Inc., 610 Main Street, Cambridge, MA 02139, USA
*Correspondence: atan.gross@weizmann.ac.il
http://dx.doi.org/10.1016/j.celrep.2016.01.046

SUMMARY

Mitochondrial carrier homolog 2 (MTCH2) is a repressor of mitochondrial oxidative phosphorylation (OXPHOS), and its locus is associated with increased BMI in humans. Here, we demonstrate that mice deficient in muscle MTCH2 are protected from diet-induced obesity and hyperinsulinemia and that they demonstrate increased energy expenditure. Deletion of muscle MTCH2 also increases mitochondrial OXPHOS and mass, triggers conversion from glycolytic to oxidative fibers, increases capacity for endurance exercise, and increases heart function. Moreover, metabolic profiling of mice deficient in muscle MTCH2 reveals a preference for carbohydrate utilization and an increase in mitochondria and glycolytic flux in muscles. Thus, MTCH2 is a critical player in muscle biology, modulating metabolism and mitochondria mass as well as impacting whole-body energy homeostasis.

INTRODUCTION

Skeletal muscle is the major body tissue that significantly increases glucose uptake following insulin stimulation. This behavior underlines the importance of muscle tissue in responding to carbohydrate availability and is suggested to play an important role in the development of whole-body insulin resistance and type 2 diabetes accompanied by obesity (Rolfe and Brown, 1997). The etiologic connection between skeletal muscle and the metabolic syndrome has been suggested to be partly due to mitochondrial dysfunction (Lowell and Shulman, 2005; Mensink et al., 2003; Mootha et al., 2003; Patti et al., 2003). Based on these observations, it was postulated that increasing mitochondrial mass/capacity in the skeletal muscle would potentially restore metabolic balance (Chan and Arany, 2014).

Mitochondrial carrier homolog 2 (MTCH2) is an uncharacterized 33-kDa protein related to members of the mitochondrial carrier protein family (Grinberg et al., 2005; Monné and Palmieri, 2014). Previously, we reported that knocking out MTCH2 in mice results in embryonic lethality at embryonic day (E)7.5, suggesting that MTCH2 plays a critical role in embryonic development (Zaltsman et al., 2010). MTCH2 is a surface-exposed outer mitochondrial membrane protein that functions as a receptor-like protein for the BH3-interacting-domain death agonist (BID) protein and is critical for Fas-induced liver apoptosis (Zaltsman et al., 2010). More recently, we found that MTCH2 functions as a repressor of mitochondria metabolism in the hematopoietic system (Maryanovich et al., 2015). Loss of MTCH2 increases mitochondrial oxidative phosphorylation (OXPHOS), triggering the entry of hematopoietic stem cells (HSC) into cycle. Moreover, elevated OXPHOS is accompanied by an increase in mitochondrial size, an increase in ATP and reactive oxygen species (ROS) levels, and protection from irradiation-induced apoptosis (Maryanovich et al., 2015).

These findings connecting MTCH2 to mitochondrial metabolism regulation relate to many recent genome-wide association studies that associate the MTCH2 locus with metabolic disorders, including diabetes and obesity (Fall et al., 2012; Heid et al., 2010; Hong and Oh, 2012; León-Mimila et al., 2013; Mei et al., 2012; van Vliet-Ostaptchouk et al., 2013; Wang et al., 2012; Willer et al., 2009). These independent studies have notably identified SNPs that might modify MTCH2 expression/function/activity. Thus, we were intrigued to find out whether MTCH2 itself acts as a metabolic regulator and whether its deregulation might lead to metabolic diseases.

To elucidate the role of MTCH2 in metabolism, we chose to study the effect of its deletion on muscle function, as well as on whole-body metabolism.

RESULTS

MTCH2$^{F/F}$*MCK-Cre*$^{+}$ Mice Are Protected from Diet-Induced Obesity and Hyperinsulinemia and Demonstrate Increased Energy Expenditure

To determine the relevance of the genome-wide association studies described earlier in an in vivo setting, we generated a

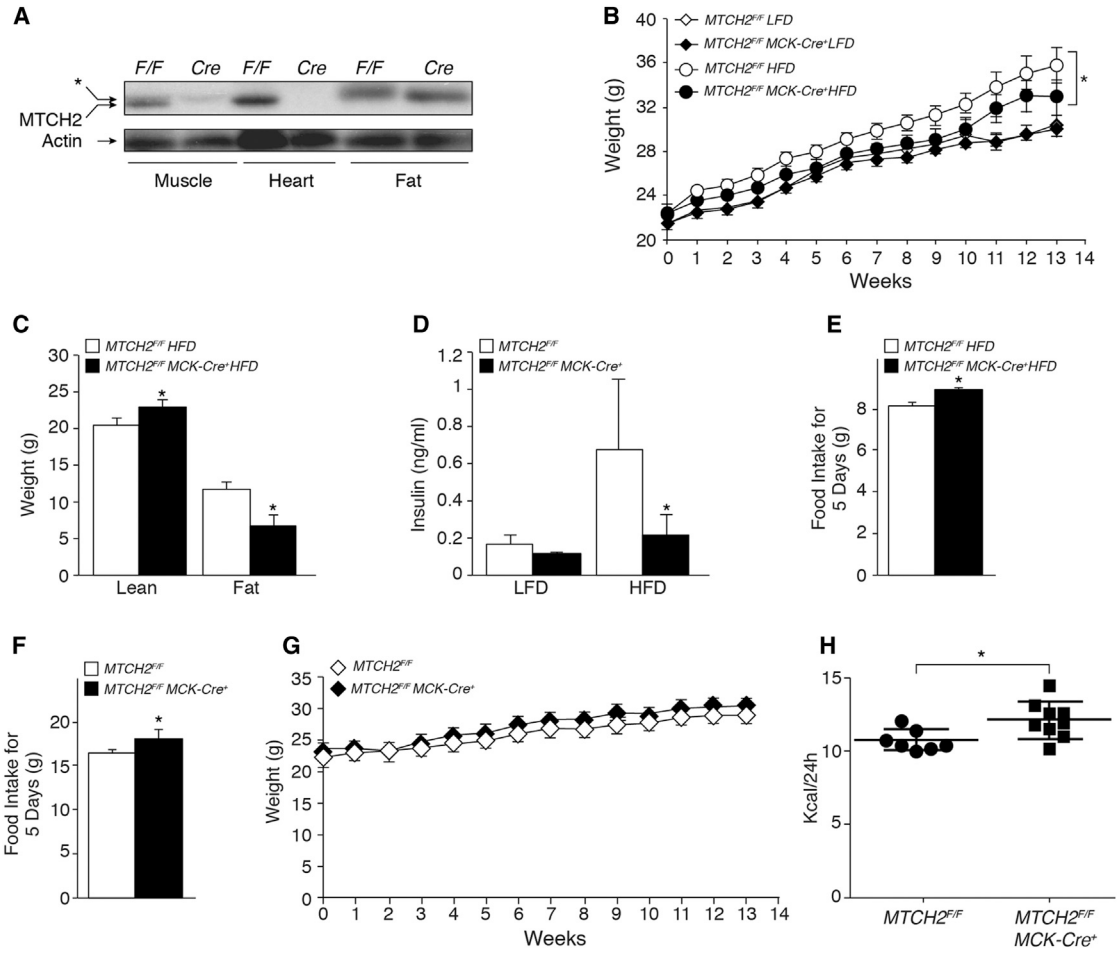

Figure 1. *MTCH2*$^{F/F}$*MCK-Cre*$^{+}$ Mice Are Protected from Diet-Induced Obesity and Hyperinsulinemia and Demonstrate Increased Energy Expenditure

(A) Specific MTCH2 knockout in skeletal muscle and heart. Western blot analysis using anti-MTCH2 antibodies of lysates prepared from skeletal muscle, heart, and fat tissue of *MTCH2*$^{F/F}$ (*F/F*) and *MTCH2*$^{F/F}$ *MCK-Cre*$^{+}$ (*Cre*) mice. The asterisk marks a crossreactive band. Actin served as a loading control.

(B) *MTCH2*$^{F/F}$ *MCK-Cre*$^{+}$ mice gain significantly less weight on a high-fat diet. The weight gains of the *MTCH2*$^{F/F}$ and *MTCH2*$^{F/F}$ *MCK-Cre*$^{+}$ littermate mice fed on a low-fat diet (LFD; 10% fat) and a high-fat diet (HFD; 45% fat) for 13 weeks are presented. The data represent mean ± SEM. *p ≤ 0.05, two-way ANOVA, n = 12 mice.

(C) *MTCH2*$^{F/F}$ *MCK-Cre*$^{+}$ mice possess less fat on an HFD. Mice, after 13 weeks on an HFD, were analyzed for the weight of their lean and fat tissues using the EchoMRI device. The data represent mean ± SEM. *p ≤ 0.05, n = 12.

(D) *MTCH2*$^{F/F}$ *MCK-Cre*$^{+}$ mice have reduced levels of plasma insulin after 13 weeks on an HFD. The data represent mean ± SD. *p ≤ 0.05, n = 9 mice.

(E) *MTCH2*$^{F/F}$ *MCK-Cre*$^{+}$ mice eat more on an HFD. Sum of 120 hr food intake measured while in the metabolic cages. The data represent mean ± SEM. *p ≤ 0.05, n = 6 mice.

(F) *MTCH2*$^{F/F}$ *MCK-Cre*$^{+}$ mice eat more on a normal chow diet. Sum of 120 hr food intake measured while in the metabolic cages. The data represent mean ± SEM. *p ≤ 0.05, n = 16 mice.

(G) *MTCH2*$^{F/F}$ *MCK-Cre*$^{+}$ mice gain similar weight as *MTCH2*$^{F/F}$ mice on a normal chow diet. The weight gains of the *MTCH2*$^{F/F}$ and *MTCH2*$^{F/F}$ *MCK-Cre*$^{+}$ littermate mice fed on a normal chow diet for 13 weeks are presented. The data represent mean ± SEM. n = 12 mice.

(H) *MTCH2*$^{F/F}$ *MCK-Cre*$^{+}$ mice demonstrate increased energy expenditure. Energy expenditure is expressed as heat production in absolute values (kilocalories per 24 hr) and statistically controlled for lean body weight. An ANCOVA was performed using a univariate general linear model module in SPSS. *p ≤ 0.05, n = 8 mice.

genetic mouse model where *MTCH2* deletion is driven by the muscle creatine kinase (MCK) Cre allele (*MTCH2*$^{F/F}$*MCK-Cre*$^{+}$) (Brüning et al., 1998), resulting in specific *MTCH2* knockout in skeletal muscle and in the heart (Figure 1A; Figure S1A). The *MTCH2*$^{F/F}$*MCK-Cre*$^{+}$ mice are viable and fertile and exhibit no obvious histological abnormalities in the skeletal muscle tissue (Figure S1B). Metabolic characterization indicates that *MTCH2*$^{F/F}$*MCK-Cre*$^{+}$ mice are less susceptible to weight gain, compared to control mice on a high-fat diet (Figure 1B). Indeed, *MTCH2*$^{F/F}$*MCK-Cre*$^{+}$ mice have less fat per body weight (Figure 1C; Figure S1C) and have lower levels of circulating insulin (Figure 1D) when fed a high-fat diet. This protection against

weight gain is not due to reduced food intake, as *MTCH2*$^{F/F}$ *MCK-Cre*$^{+}$ mice eat more than their control littermates on a high-fat diet (Figure 1E). Also, on a regular chow diet, the *MTCH2*$^{F/F}$*MCK-Cre*$^{+}$ mice eat more (Figure 1F) but do not gain more weight (Figure 1G) and show the same body composition (Figure S1D). Importantly, the *MTCH2*$^{F/F}$*MCK-Cre*$^{+}$ mice demonstrate an increase in energy expenditure (Figure 1H; Figure S1E), suggesting that loss of MTCH2 leads to an increase in whole-body energy utilization.

Deletion of MTCH2 in Muscle Increases Mitochondrial OXPHOS and Mass

To characterize MTCH2 deletion impact on muscle morphology and function, we performed electron microscopy (EM) analyses on the gastrocnemius muscles (a mixed muscle mostly composed of glycolytic fibers). The analysis revealed a striking increase in mitochondrial area in the *MTCH2*$^{F/F}$*MCK-Cre*$^{+}$ muscles compared to muscles in the control littermates (Figure 2A). MTCH2-deficient muscles also showed an increase in mtDNA (Figure 2B), accompanied by increased expression of the respiratory complexes (Figure 2C).

To define the functional consequence of MTCH2 deletion on skeletal muscle cell mitochondria, myotubes from *MTCH2*$^{F/F}$ mice (Zaltsman et al., 2010) were left untreated or transduced with purified Cre recombinase (Figure 2D), and cellular respiration was measured. Loss of MTCH2 led to an increase in basal and maximal oxygen consumption (Figure 2E, left and right panels) and to an increase in mitochondrial mass (Figure 2F). We also measured respiration using isolated skeletal muscle mitochondria and found no differences between the *MTCH2*$^{F/F}$ and *MTCH2*$^{F/F}$*MCK-Cre*$^{+}$ (Figure S2A), suggesting that the increased respiration in intact cells is likely due to an increase in mitochondrial mass. As an initial attempt to assess how lack of MTCH2 leads to an increase in mitochondrial mass, we assessed the expression levels of the major factors involved in mitochondrial biogenesis, mitochondrial dynamics, and autophagy but found no significant differences between the *MTCH2*$^{F/F}$ and *MTCH2*$^{F/F}$ *MCK-Cre*$^{+}$ samples (Figures S2B–S2D, respectively).

Taken together, MTCH2 deletion in skeletal muscle results in a direct increase in mitochondrial OXPHOS and mass, suggesting that MTCH2 acts as a repressor of muscle mitochondrial mass/function.

Deletion of Muscle MTCH2 Triggers Conversion from Glycolytic to Oxidative Fibers, Increases the Capacity for Endurance Exercise, and Increases Heart Function

Next, we assessed the effect of increased mitochondrial mass/function on muscle physiology and started with the muscle fibers' type pattern. Consistent with previous studies (Lin et al., 2002), we found in *MTCH2*$^{F/F}$*MCK-Cre*$^{+}$ gastrocnemius muscle, where mitochondrial OXPHOS content was elevated, a significant increase in the oxidative myosin heavy chain 1 (MHC1; type I) fibers and decrease in MHC2b (type IIB) fibers (Figure 3A, left and right panels). Although the muscle fiber distribution was changed (from glycolytic to more oxidative), the basal activity of the *MTCH2*$^{F/F}$*MCK-Cre*$^{+}$ mice remained similar to that of their wild-type littermates (Figure S3A). However, a forced-endurance exercise test (with a predetermined ceiling of 425 m) demonstrated that *MTCH2*$^{F/F}$*MCK-Cre*$^{+}$ mice performed better than their *MTCH2*$^{F/F}$ littermates (Figure 3B) and consumed more oxygen during this exercise profile (Figure 3C).

MTCH2 protein is as prevalent in heart as in skeletal muscle, and the MCK-Cre leads to deletion of MTCH2 in both skeletal and cardiac muscle (Figure 1A). Therefore, next, we performed an echocardiographic analysis and found that loss of muscle MTCH2 increases heart function (stroke volume, ejection fraction, and fractional shortening; Figures 3D–3F, respectively), with no significant change in heart size (Figures S3B–S3D). Thus, these results suggest that the increase in heart function is likely to contribute to the improved endurance performance observed in the *MTCH2*$^{F/F}$*MCK-Cre*$^{+}$ mice (Figure 3B). We also used the heart tissue to perform electron microscopy (EM) analysis (to determine the mitochondrial area) and to measure the levels of mtDNA, and, in both analyses, we found no significant differences between the *MTCH2*$^{F/F}$ and *MTCH2*$^{F/F}$ *MCK-Cre*$^{+}$ samples (Figures S3E and S3F, respectively).

Taken together, MTCH2 deletion in muscle results in an increase in oxidative fibers and in heart function, and both are likely to contribute to the increases in capacity for endurance exercise.

Loss of Muscle MTCH2 Leads to Preference for Carbohydrate Utilization and Increases Mitochondria and Glycolytic Flux in Muscle

Next, we investigated whether MTCH2 deletion in muscle would perturb whole-body energy utilization. *MTCH2*$^{F/F}$*MCK-Cre*$^{+}$ respiratory exchange ratio (RER) is comparable to that of control littermates upon basal feeding conditions. Differences became apparent at the beginning of a fast. While the control mice showed a significant decrease in RER, as expected, the *MTCH2*$^{F/F}$*MCK-Cre*$^{+}$ RER dropped as well, but to a lesser extent than that of the control mice (Figure 4A). To further characterize those metabolic changes, we performed metabolomics and lipidomics profiling of the plasma of the fed and 24-hr-fasted mice. Interestingly, circulating lactate levels were elevated in the fed *MTCH2*$^{F/F}$*MCK-Cre*$^{+}$ mice (Figure 4B), which was not apparent in the plasma of 24-hr-fasted *MTCH2*$^{F/F}$ control mice. Tricarboxylic-acid (TCA)-cycle intermediate levels (fumarate, malate, and α-ketoglutarate) follow the circulating lactate pattern and are elevated as well in the *MTCH2*$^{F/F}$*MCK-Cre*$^{+}$ mice, as compared to those of their control littermates in the fed state (Figure 4C). These results suggest a higher glycolytic flux and oxidation rate. These metabolic differences between the two groups disappeared when both groups were subjected to 24-hr starvation.

Lipidomics analysis revealed some subtle changes. Circulating triacylglycerol (TAG) and diacylglycerol (DAG) levels dropped upon starvation, as expected in both groups, compared to those in the fed state (Figures S4A and S4B). The circulating *MTCH2*$^{F/F}$*MCK-Cre*$^{+}$ TAG and DAG levels are similar when compared to those of the *MTCH2*$^{F/F}$ control group in both the fed and starved states. Even though circulating *MTCH2*$^{F/F}$*MCK-Cre*$^{+}$ TAGs and DAGs are equivalent to *MTCH2*$^{F/F}$ TAGs and DAGs, subtle but significant changes can be observed in specific

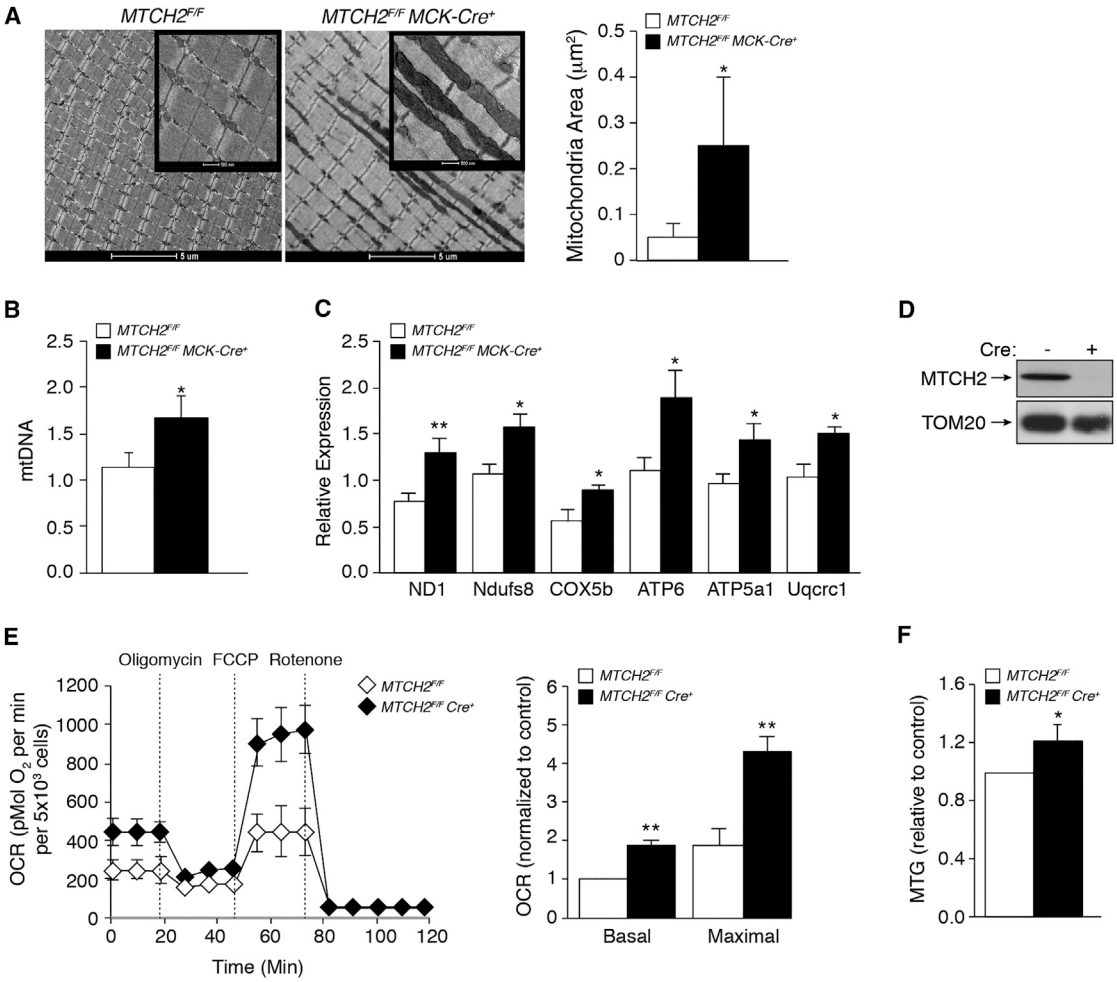

Figure 2. Deletion of MTCH2 in Muscle Increases Mitochondrial OXPHOS and Mass

(A) Loss of MTCH2 leads to an increase in the mitochondrial area in gastrocnemius muscles. Left panels: representative EM images are presented (1900× and 9300× magnifications; scale bars, 5 μm and 500 nm, respectively). Right panel: analysis of mitochondrial area. The data represent mean ± SEM. *p ≤ 0.05.

(B) Increased mtDNA abundance in *MTCH2$^{F/F}$ MCK-Cre^{+}* gastrocnemius muscle. mtDNA was measured by real-time PCR using *ChrM* and *COX1* (mitochondrial-encoded genes) expressed relative to *HPRT*, a housekeeping gene. *Glucagon* served as the control nuclear-encoded gene. The data represent mean ± SEM. *p ≤ 0.05, n = 8 mice.

(C) Elevated expression of nuclear- and mitochondrial-encoded mitochondrial respiratory complex subunits in *MTCH2$^{F/F}$ MCK-Cre^{+}* gastrocnemius muscle. Relative gene expression was evaluated by real-time PCR and normalized to *HPRT* expression. Results are presented as mean relative expression ± SEM. *p ≤ 0.05; **p ≤ 0.01, n = 8 mice.

(D) Representative western blot using anti-MTCH2 antibodies of enriched mitochondrial fractions of myotubes isolated from *MTCH2$^{F/F}$* mice either left untreated (−) or treated (+) with recombinant Cre recombinase. TOM20 serves as a mitochondrial fraction loading control.

(E) Loss of MTCH2 results in increased mitochondrial respiration in myotubes. Left panel: OCRs were measured using the Seahorse XF24 analyzer under basal conditions and in response to 1.5 μM oligomycin (complex V inhibitor), 4 μM FCCP (uncoupler), or 2 μM Rotenone (complex I inhibitor). A representative tracing of a typical experiment set of four is shown. Right panel: normalized average of results shown in the left panel; Basal and maximal OCRs (as indicated by OCR before injection of oligomycin and subsequent FCCP). The data represent mean ± SD. **p ≤ 0.01.

(F) Loss of MTCH2 results in an increase in mitochondrial mass. Myotubes were assessed for mitochondria mass using Mito Tracker Green (MTG) as described in the Supplemental Experimental Procedures. Data are presented as mean ± SEM. *p ≤ 0.05, n = 4.

lipids species, such as decreased 16:0-20:4-20:4 and 18:2-18:2-20:4 (TAGs) and 16:0-20:5 and 18:0-16:0 (DAGs) (Figures S4C and S4D, respectively). As the *MTCH2$^{F/F}$MCK-Cre^{+}* RER suggested a lower capacity to oxidize fat, we investigated circulating levels of long-chain acylcarnitine (AC) pool. Fasting conditions increased AC content to a similar extent in the *MTCH2$^{F/F}$* and *MTCH2$^{F/F}$MCK-Cre^{+}* groups (Figure S4E), suggesting that MTCH2-deleted muscle is also capable of utilizing fatty acids as substrate for oxidation. Thus, MTCH2 muscle-specific knockout mice maintain fatty acid oxidation capacity but do exhibit carbohydrate substrate preference, suggesting a role for MTCH2 in metabolic control.

To determine whether changes in circulating metabolites are reflecting changes in the muscle metabolites' pattern upon

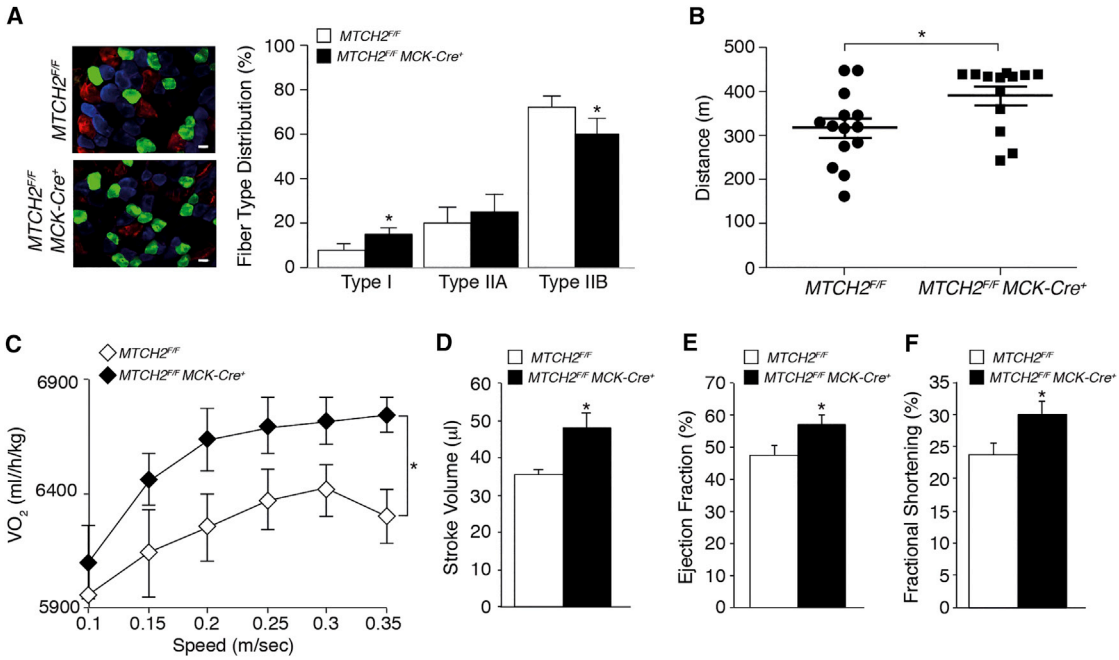

Figure 3. Deletion of Muscle MTCH2 Triggers Conversion from Glycolytic to Oxidative Fibers, Increases Capacity for Endurance Exercise, and Increases Heart Function

(A) Loss of MTCH2 triggers conversion from glycolytic to oxidative fibers. Left panels: representative images of immunostaining of *MTCH2$^{F/F}$* and *MTCH2$^{F/F}$ MCK-Cre^{+}* gastrocnemius muscles. The staining discriminates and reveals the relative abundance of MHC type I (green), IIA (blue), and IIB (red) fibers. Images are presented at a 40× magnification; scale bars indicate 20 μm. Right: comparison of muscle fiber type percent distribution between *MTCH2$^{F/F}$* and *MTCH2$^{F/F}$ MCK-Cre^{+}* gastrocnemius muscles. The data represent mean ± SEM. *p ≤ 0.05, n = 3 mice.

(B) Loss of MTCH2 increases distance covered by the mice during exercise until exhaustion. *MTCH2$^{F/F}$* and *MTCH2$^{F/F}$ MCK-Cre^{+}* mice underwent an exhaustion protocol on the treadmill, as described in the Supplemental Experimental Procedures. The data represent mean ± SEM. *p ≤ 0.05, n = 15 mice.

(C) Loss of MTCH2 increases oxygen consumption during the exhaustion profile exercise. The data represent mean ± SEM. *p ≤ 0.05, n = 16 mice; two-way ANOVA.

(D–F) Loss of MTCH2 increases heart function. Echocardiographic analysis shows an increase in heart function measurements of *MTCH2$^{F/F}$ MCK-Cre^{+}* mice, as compared to *MTCH2$^{F/F}$* mice, in stroke volume (D), ejection fraction (E), and fractional shortening (F). The data represent mean ± SEM. *p ≤ 0.05, n = 5 mice.

MTCH2 loss, we performed metabolic profiling of the gastrocnemius muscles and the soleus muscles (a muscle type mostly composed of oxidative fibers). The muscles were prepared from mice either fed or fasted for 24 hr, since it is well established that fasting increases mitochondrial metabolism (de Lange et al., 2007). Strikingly, the soleus muscles of the fed *MTCH2$^{F/F}$ MCK-Cre^{+}* mice showed a significant increase in the glycolysis metabolite pyruvate (Figure 4D) and the TCA-cycle metabolite malate (Figure 4E), which was similar to the increase in both metabolites in the soleus muscles of the 24-hr-fasted *MTCH2$^{F/F}$* control mice (Figures 4D and 4E, respectively). Notably, a 24-hr fast of the *MTCH2$^{F/F}$* control mice also increased the levels of fumarate (TCA cycle) and lactate (glycolysis), and a similar trend was seen in fed *MTCH2$^{F/F}$MCK-Cre^{+}* mice (Figures 4E and 4F, respectively). The gastrocnemius muscles of the fed *MTCH2$^{F/F}$MCK-Cre^{+}* mice also showed a similar trend of an increase in glycolysis and TCA-cycle metabolites (Figures S5A and S5B, respectively).

Simultaneously, glucose uptake is increased in *MTCH2$^{F/F}$-Cre^{+}* primary myotubes (Figure S5C), while *MTCH2$^{F/F}$MCK-Cre^{+}* muscle glycogen content is also elevated when compared to that in control muscle (Figure S5D). This suggests that loss of MTCH2 leads to an increase in mitochondria and glycolytic flux but that the excess of carbohydrate is not fully oxidized and stored in glycogen form. Meanwhile, lower muscle TAGs and DAG levels, and increased AC (Figures S5E–S5G, respectively), are found upon starvation in both mouse groups, as expected. However, there were no significant differences between the muscle lipid profiles of the *MTCH2$^{F/F}$* and *MTCH2$^{F/F}$MCK-Cre^{+}* mice, mimicking the circulating organic acids' and lipids' profile results.

Collectively, we demonstrate that MTCH2 muscle-specific deletion increases mitochondrial metabolism and mass, which results in increased muscle metabolic capacity, increased energy demand and expenditure, and whole-body protection from diet-induced obesity (Figure 4G).

DISCUSSION

In the present study, we demonstrate that MTCH2 is a critical player in muscle biology, modulating mitochondrial mass and its metabolism with a significant impact on whole-body energy homeostasis.

Many recent genome-wide association studies have associated the MTCH2 locus with metabolic disorders, including diabetes and obesity, suggesting that MTCH2 deregulation might

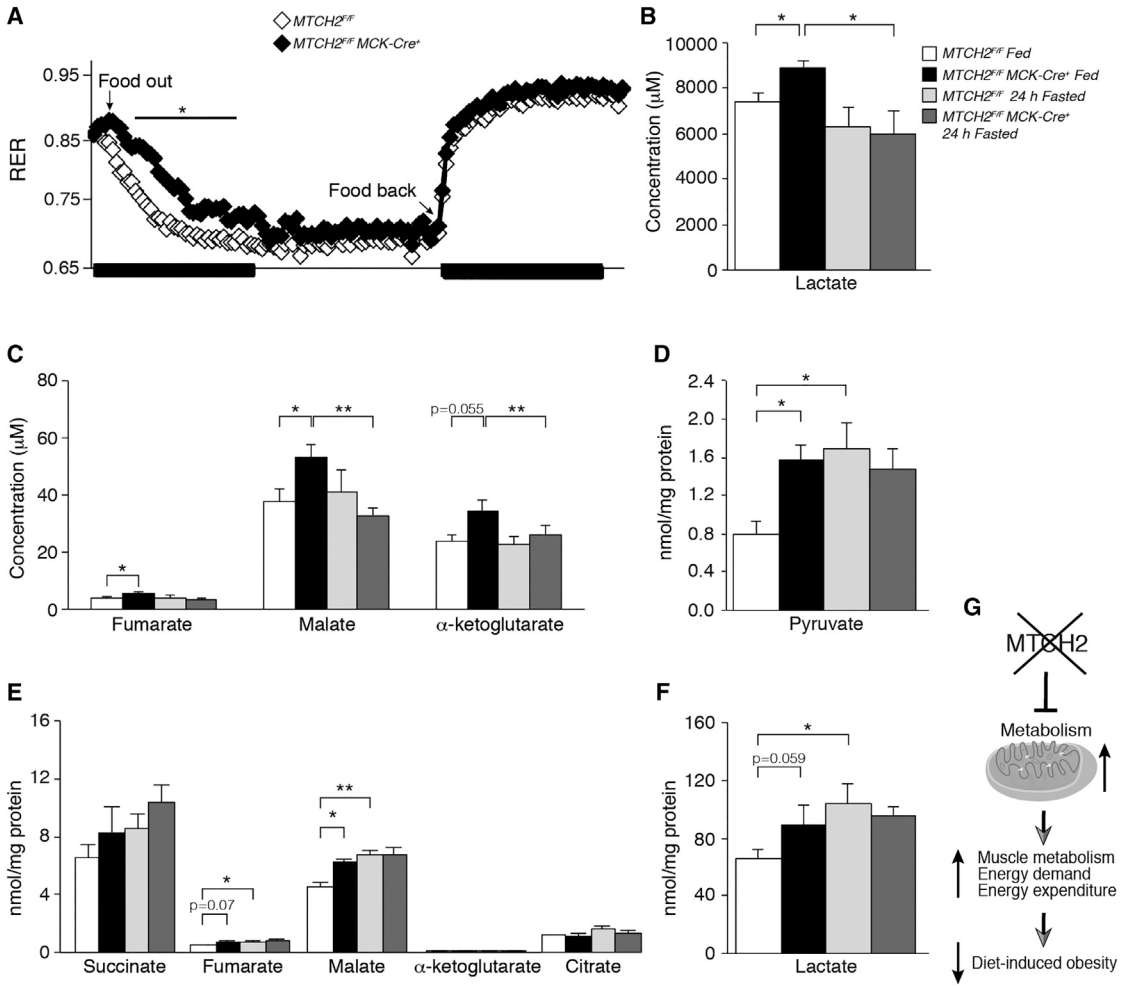

Figure 4. Loss of Muscle MTCH2 Leads to Preference for Carbohydrate Utilization and Increases Mitochondria and Glycolytic Flux in Muscle

(A) *MTCH2*$^{F/F}$ *MCK-Cre*$^{+}$ mice maintain a higher RER under fasting conditions. Metabolic cages were used to measure RER during fasting (Food out) and re-feeding (Food back) in the *MTCH2*$^{F/F}$ and *MTCH2*$^{F/F}$ *MCK-Cre*$^{+}$ mice. The black thick lines at the bottom of the graph represent the 12-hr dark periods. The data represent mean ± SEM. *p $\leq$ 0.05, n = 16 mice.

(B and C) Metabolic profiling of plasma prepared from fed and 24-hr-fasted *MTCH2*$^{F/F}$ and *MTCH2*$^{F/F}$ *MCK-Cre*$^{+}$ mice using LC/MS/MS, showing a significant increase in lactate (B), and in fumarate and malate (C), whereas the plasma from 24-hr-fasted *MTCH2*$^{F/F}$ mice does not show such an increase. The data represent mean ± SEM. *p $\leq$ 0.05; **p $\leq$ 0.01, n = 5 mice for each treatment.

(D–F) Metabolic profiling of soleus muscles prepared from fed and 24-hr-fasted *MTCH2*$^{F/F}$ and *MTCH2*$^{F/F}$ *MCK-Cre*$^{+}$ mice using LC/MS/MS. *MTCH2*$^{F/F}$ *MCK-Cre*$^{+}$ muscles prepared from fed mice demonstrate a significant increase in pyruvate (D) and malate (E), similar to the increase in the 24-hr-fasted *MTCH2*$^{F/F}$ mice. 24-hr-fasted *MTCH2*$^{F/F}$ mice demonstrated a significant increase in lactate (F), which is not significantly increased in the fed *MTCH2*$^{F/F}$ *MCK-Cre*$^{+}$ mice. The data represent mean ± SEM. *p $\leq$ 0.05; **p $\leq$ 0.01, n = 5 mice for each treatment.

(G) Schematic representation of the effect of muscle MTCH2 deletion on mitochondria and muscle metabolism, energy demand and expenditure, and whole-body protection from diet-induced obesity.

lead to metabolic disease. In this study, we indeed found that MTCH2 deficiency in muscle is beneficial, protecting mice from a high-fat diet, and that this protection is most likely due to the increase in mitochondria and muscle metabolism, leading to elevated whole-body energy demand and elevated energy expenditure.

Related to these findings are several previous studies that have postulated that increasing mitochondrial mass in the skeletal muscle via expression of PPARγ coactivator 1-α (PGC-1α) would potentially improve metabolic syndrome (Chan and Arany, 2014). However, muscle-specific overexpression of PGC-1α in mice did not improve whole-body glucose homeostasis in the sedentary state; rather, it induced peripheral insulin resistance on a high-fat diet (Choi et al., 2008). Interestingly, however, as opposed to the sedentary state, when exercised, the PGC-1α-muscle transgenic mice reversed this phenotype and displayed increased insulin sensitivity (Summermatter et al., 2013).

Importantly, our studies reveal that loss of muscle MTCH2, which leads to an increase in mitochondrial mass/function, is sufficient to slow down body weight gain on a high-fat diet and

protect from hyperinsulinemia without the requirement of triggered exercise. Moreover, circulating lactate and TCA-cycle intermediate levels were elevated in the fed *MTCH2*$^{F/F}$*MCK-Cre*$^{+}$ mice. Since others have reported that lactate and TCA-cycle intermediate levels are increased following exercise in humans (Lewis et al., 2010), it may be speculated that the *MTCH2*$^{F/F}$ *MCK-Cre*$^{+}$ mice phenocopy an exercised state.

The *MTCH2*$^{F/F}$*MCK-Cre*$^{+}$ mice eat more on regular chow and high-fat diets. Simultaneously, loss of MTCH2 increases glucose uptake and glycogen storage and, under fasting conditions, maintains carbohydrate metabolism. These results are consistent with the idea that *MTCH2*$^{F/F}$*MCK-Cre*$^{+}$ mice are in a constant state of increased carbohydrate utilization, but, as the elevated AC level upon fasting demonstrates, these mice have retained fatty acid oxidation capacity.

In accordance with the aforementioned findings, the MTCH2-deficient muscles under fed conditions showed increases in pyruvate and malate that were similar to the increases seen in the 24-hr-fasted control muscles. Most likely, the increase in these metabolites represents an increase in their storage, since the organism cannot rely on obtaining food from external sources and shifts to depending solely on its internal sources. Notably, a 24-hr fast of the MTCH2-deficient mice did not further increase the levels of either glycolysis or TCA-cycle intermediates, suggesting that loss of MTCH2 results in a maximal metabolic response in the muscles. Thus, MTCH2 acts as a critical repressor of muscle metabolism, and once it is lost, both forms of energy production—glycolysis and OXPHOS—are upregulated.

As mentioned in the Introduction, we initially characterized MTCH2 as a receptor-like protein for pro-apoptotic BID (Zaltsman et al., 2010). Interestingly, several pro-apoptotic proteins residing at mitochondria—BAD, AIF, and Noxa—have been recently demonstrated to also play a role in regulating glucose metabolism (Giménez-Cassina et al., 2014; Lowman et al., 2010; Pospisilik et al., 2007). Notably, muscle- and liver-specific deletion of AIF improves glucose tolerance and insulin sensitivity and protects from diet-induced obesity (Pospisilik et al., 2007), and a BAD phosphomimic variant counteracting unrestrained gluconeogenesis improves glycemia in leptin-resistant and high-fat-diet models of diabetes and insulin resistance (Giménez-Cassina et al., 2014). Thus, the homeostatic crosstalk between glucose metabolism and apoptosis seems to be governed by shared regulatory components (Giménez-Cassina and Danial, 2015). In the context of our study, it remains to be determined whether BID is the upstream metabolic regulator of MTCH2.

In summary, we have identified mitochondrial MTCH2 as a pivotal regulator of muscle metabolism and whole-body energy homeostasis. Our findings represent an advance in establishing the connection between mitochondrial function and obesity, with a potentially important contribution to our understanding of metabolic diseases in humans.

EXPERIMENTAL PROCEDURES

Mice

The Weizmann Institute Animal Care and Use Committee approved all animal experiments. *MTCH2*$^{F/F}$ mice were generated as described previously (Zaltsman et al., 2010). MCK-Cre mice (on a pure C57BL/6 background) were purchased from Jackson Laboratory (stock #006475). In vivo assays were repeated in at least three independent experiments with 10- to 14-week-old littermate male mice. Mice were housed in a reversed-cycle condition of 12 hr/12 hr dark/light, and all experiments were performed in the dark phase of the day cycle. Mice were fed on a normal chow diet: 17% of kilocalories from fat and 58% from carbohydrates (total, 3.1 kcal/g).

Metabolic Cages

Indirect calorimetry and food intake, as well as locomotor activity, were measured using the LabMaster system (TSE Systems). The calorimetry system is an open-circuit system that determines O_2 consumption, CO_2 production, and RER. Data were collected after 48 hr of adaptation in acclimated singly housed mice. Immediately following the measurements of their basal metabolic parameters, mice were deprived of food for 20 hr while in the LabMaster system. Heat production was adjusted to lean mass using an ANCOVA (Tschöp et al., 2012).

High-Fat Diet

Weight-matched experimental littermate mice were fed for 13 weeks with a high-fat diet (45% of kilocalories from fat, and 35% from carbohydrates; total, 4.7 kcal/g; catalog #D12451, Research Diets) or a low-fat diet (10% of kilocalories from fat and 70% from carbohydrates; total, 3.8 kcal/g; catalog #D12450B, Research Diets) as a cohort control. Body weights were monitored every week during the diet. Insulin levels were measured in the serum using an insulin kit (catalog #90080, Crystal Chem).

Metabolic Profiling

Muscles and plasma of fed and 24-hr-fasted mice were assayed for organic acids at the Sanford Burnham Medical Research Institute (SBMRI) Metabolomics Core. Tissues were lyophilized and subsequently ground into a fine powder using an automated bead-based tissue homogenizer (Precellys Evolution; Bertin Corporation). Tissues and plasma were assayed for organic acids using Thermo Quantiva liquid chromatography/tandem mass spectrometry (LC/MS/MS) instruments, and authentic heavy isotope-labeled internal standards were used for all organic acids.

Muscle Cell Respiration

MTCH2$^{F/F}$ and *MTCH2*$^{F/F}$*-Cre*$^{+}$ myotubes were seeded in XF24 plates (catalog #100777-004, Seahorse Bioscience). Measurement of intact cellular respiration was performed using the Seahorse XF24 analyzer (Seahorse Bioscience). Oxygen consumption rates (OCRs) (picomoles of O_2 per minute) were measured under basal conditions and after three consecutive injections of the following: (1) oligomycin (ATP synthase inhibitor; 1.5 μM); (2) the electron transport chain accelerator ionophore FCCP (5 μM; FCCP treatment gives the maximal OCR capacity of the cells); and (3) the electron transport chain inhibitor rotenone (2 μM), which stops respiration.

Transmission EM

Gastrocnemius muscles and hearts were dissected and placed in relaxation buffer (Fawcett and McNutt, 1969) for 3 min. Next, samples were fixed with 3% paraformaldehyde, 2% glutaraldehyde in 0.1 M cacodylate buffer containing 5 mM $CaCl_2$ (pH 7.4). Next, samples were post-fixated in 1% osmium tetroxide supplemented with 0.5% potassium hexacyanoferrate tryhidrate and potasssium dichromate in 0.1 M cacodylate (1 hr), stained with 2% uranyl acetate in water (1 hr), dehydrated in graded ethanol solutions, and embedded in Agar 100 epoxy resin (Agar Scientific). Ultrathin longitudinal sections (70–90 nm) were viewed and photographed with a Tecnai Spirit (FEI) transmission electron microscope operated at 120 kV and equipped with an Eagle CCD (charge-coupled device) camera. Random fields were chosen, and the mitochondrial area was measured per total area using ImageJ software.

Statistical Analysis

The p values were calculated by using an unpaired Student's t test.

SUPPLEMENTAL INFORMATION

Supplemental Information includes Supplemental Experimental Procedures and five figures and can be found with this article online at http://dx.doi.org/10.1016/j.celrep.2016.01.046.

AUTHOR CONTRIBUTIONS

L.B.-A. performed most of the experiments and analyzed all the data presented in the manuscript. Y.K. was a consultant on the metabolic experiments and performed part of the analysis. M.T. was a consultant on the behavior experiments. Y.Z. helped in performing part of the experiments, and L.S. generated the *MTCH2*$^{F/F}$ mice. S.L.Z. performed the EM studies, and E.B. performed the echocardiographic analysis. I.M. helped with the fiber-typing studies, and A.S. helped with the echocardiogram (ECG) studies. E.T. was a consultant on the heart measurements, M.H was a consultant in several experiments, and C.V. coordinated the metabolomics and lipidomics profiling and helped in writing the manuscript. L.B.-A. and A.G. conceived the ideas, planned the projects, and wrote the manuscript. All authors discussed the results and commented on the manuscript.

ACKNOWLEDGMENTS

We are grateful to Alon Harmelin, Rebecca Haffner, Alina Maizenberg, Golda Damari, and Calanit Raanan for help with generating the *MTCH2*$^{F/F}$ mice. We also thank Sharon Ovadia, Dalia Vaknin, Nava Nevo, Inbal Biton, and Yuri Kuznetsov for help with animal studies, and Helena Sabanay for help with EM studies. This study was supported in part by the Israel Science Foundation (ISF), USA-Israel Binational Science Foundation (BSF), German-Israel Foundation (GIF), Minerva Stiftung, and a Hyman T. Milgrom Trust grant. A.G. is the incumbent of the Marketa and Frederick Alexander Professorial Chair.

Received: August 11, 2015
Revised: December 1, 2015
Accepted: January 13, 2016
Published: February 11, 2016

REFERENCES

Brüning, J.C., Michael, M.D., Winnay, J.N., Hayashi, T., Hörsch, D., Accili, D., Goodyear, L.J., and Kahn, C.R. (1998). A muscle-specific insulin receptor knockout exhibits features of the metabolic syndrome of NIDDM without altering glucose tolerance. Mol. Cell *2*, 559–569.

Chan, M.C., and Arany, Z. (2014). The many roles of PGC-1α in muscle–recent developments. Metabolism *63*, 441–451.

Choi, C.S., Befroy, D.E., Codella, R., Kim, S., Reznick, R.M., Hwang, Y.-J., Liu, Z.-X., Lee, H.-Y., Distefano, A., Samuel, V.T., et al. (2008). Paradoxical effects of increased expression of PGC-1α on muscle mitochondrial function and insulin-stimulated muscle glucose metabolism. Proc. Natl. Acad. Sci. USA *105*, 19926–19931.

de Lange, P., Moreno, M., Silvestri, E., Lombardi, A., Goglia, F., and Lanni, A. (2007). Fuel economy in food-deprived skeletal muscle: signaling pathways and regulatory mechanisms. FASEB J. *21*, 3431–3441.

Fall, T., Arnlöv, J., Berne, C., and Ingelsson, E. (2012). The role of obesity-related genetic loci in insulin sensitivity. Diabet. Med. *29*, e62–e66.

Fawcett, D.W., and McNutt, N.S. (1969). The ultrastructure of the cat myocardium. I. Ventricular papillary muscle. J. Cell Biol. *42*, 1–45.

Giménez-Cassina, A., and Danial, N.N. (2015). Regulation of mitochondrial nutrient and energy metabolism by BCL-2 family proteins. Trends Endocrinol. Metab. *26*, 165–175.

Giménez-Cassina, A., Garcia-Haro, L., Choi, C.S., Osundiji, M.A., Lane, E.A., Huang, H., Yildirim, M.A., Szlyk, B., Fisher, J.K., Polak, K., et al. (2014). Regulation of hepatic energy metabolism and gluconeogenesis by BAD. Cell Metab. *19*, 272–284.

Grinberg, M., Schwarz, M., Zaltsman, Y., Eini, T., Niv, H., Pietrokovski, S., and Gross, A. (2005). Mitochondrial carrier homolog 2 is a target of tBID in cells signaled to die by tumor necrosis factor alpha. Mol. Cell. Biol. *25*, 4579–4590.

Heid, I.M., Jackson, A.U., Randall, J.C., Winkler, T.W., Qi, L., Steinthorsdottir, V., Thorleifsson, G., Zillikens, M.C., Speliotes, E.K., Mägi, R., et al.; MAGIC (2010). Meta-analysis identifies 13 new loci associated with waist-hip ratio and reveals sexual dimorphism in the genetic basis of fat distribution. Nat. Genet. *42*, 949–960.

Hong, K.W., and Oh, B. (2012). Recapitulation of genome-wide association studies on body mass index in the Korean population. Int. J. Obes. *36*, 1127–1130.

León-Mimila, P., Villamil-Ramírez, H., Villalobos-Comparán, M., Villarreal-Molina, T., Romero-Hidalgo, S., López-Contreras, B., Gutiérrez-Vidal, R., Vega-Badillo, J., Jacobo-Albavera, L., Posadas-Romeros, C., et al. (2013). Contribution of common genetic variants to obesity and obesity-related traits in mexican children and adults. PLoS ONE *8*, e70640.

Lewis, G.D., Farrell, L., Wood, M.J., Martinovic, M., Arany, Z., Rowe, G.C., Souza, A., Cheng, S., McCabe, E.L., Yang, E., et al. (2010). Metabolic signatures of exercise in human plasma. Sci. Transl. Med. *2*, 33ra37.

Lin, J., Wu, H., Tarr, P.T., Zhang, C.-Y., Wu, Z., Boss, O., Michael, L.F., Puigserver, P., Isotani, E., Olson, E.N., et al. (2002). Transcriptional co-activator PGC-1 alpha drives the formation of slow-twitch muscle fibres. Nature *418*, 797–801.

Lowell, B.B., and Shulman, G.I. (2005). Mitochondrial dysfunction and type 2 diabetes. Science *307*, 384–387.

Lowman, X.H., McDonnell, M.A., Kosloske, A., Odumade, O.A., Jenness, C., Karim, C.B., Jemmerson, R., and Kelekar, A. (2010). The proapoptotic function of Noxa in human leukemia cells is regulated by the kinase Cdk5 and by glucose. Mol. Cell *40*, 823–833.

Maryanovich, M., Zaltsman, Y., Ruggiero, A., Goldman, A., Shachnai, L., Zaidman, S.L., Porat, Z., Golan, K., Lapidot, T., and Gross, A. (2015). An MTCH2 pathway repressing mitochondria metabolism regulates haematopoietic stem cell fate. Nat. Commun. *6*, 7901.

Mei, H., Chen, W., Jiang, F., He, J., Srinivasan, S., Smith, E.N., Schork, N., Murray, S., and Berenson, G.S. (2012). Longitudinal replication studies of GWAS risk SNPs influencing body mass index over the course of childhood and adulthood. PLoS ONE *7*, e31470.

Mensink, M., Blaak, E.E., Vidal, H., De Bruin, T.W.A., Glatz, J.F.C., and Saris, W.H.M. (2003). Lifestyle changes and lipid metabolism gene expression and protein content in skeletal muscle of subjects with impaired glucose tolerance. Diabetologia *46*, 1082–1089.

Monné, M., and Palmieri, F. (2014). Antiporters of the mitochondrial carrier family. Curr. Top. Membr. *73*, 289–320.

Mootha, V.K., Lindgren, C.M., Eriksson, K.-F., Subramanian, A., Sihag, S., Lehar, J., Puigserver, P., Carlsson, E., Ridderstråle, M., Laurila, E., et al. (2003). PGC-1alpha-responsive genes involved in oxidative phosphorylation are coordinately downregulated in human diabetes. Nat. Genet. *34*, 267–273.

Patti, M.E., Butte, A.J., Crunkhorn, S., Cusi, K., Berria, R., Kashyap, S., Miyazaki, Y., Kohane, I., Costello, M., Saccone, R., et al. (2003). Coordinated reduction of genes of oxidative metabolism in humans with insulin resistance and diabetes: Potential role of PGC1 and NRF1. Proc. Natl. Acad. Sci. USA *100*, 8466–8471.

Pospisilik, J.A., Knauf, C., Joza, N., Benit, P., Orthofer, M., Cani, P.D., Ebersberger, I., Nakashima, T., Sarao, R., Neely, G., et al. (2007). Targeted deletion of AIF decreases mitochondrial oxidative phosphorylation and protects from obesity and diabetes. Cell *131*, 476–491.

Rolfe, D.F., and Brown, G.C. (1997). Cellular energy utilization and molecular origin of standard metabolic rate in mammals. Physiol. Rev. *77*, 731–758.

Summermatter, S., Shui, G., Maag, D., Santos, G., Wenk, M.R., and Handschin, C. (2013). PGC-1α improves glucose homeostasis in skeletal muscle in an activity-dependent manner. Diabetes *62*, 85–95.

Tschöp, M.H., Speakman, J.R., Arch, J.R., Auwerx, J., Brüning, J.C., Chan, L., Eckel, R.H., Farese, R.V., Jr., Galgani, J.E., Hambly, C., et al. (2012). A guide to analysis of mouse energy metabolism. Nat. Methods *9*, 57–63.

van Vliet-Ostaptchouk, J.V., den Hoed, M., Luan, J., Zhao, J.H., Ong, K.K., van der Most, P.J., Wong, A., Hardy, R., Kuh, D., van der Klauw, M.M., et al. (2013). Pleiotropic effects of obesity-susceptibility loci on metabolic traits: a meta-analysis of up to 37,874 individuals. Diabetologia *56*, 2134–2146.

Wang, J., Mei, H., Chen, W., Jiang, Y., Sun, W., Li, F., Fu, Q., and Jiang, F. (2012). Study of eight GWAS-identified common variants for association with obesity-related indices in Chinese children at puberty. Int. J. Obes. *36*, 542–547.

Willer, C.J., Speliotes, E.K., Loos, R.J., Li, S., Lindgren, C.M., Heid, I.M., Berndt, S.I., Elliott, A.L., Jackson, A.U., Lamina, C., et al.; Wellcome Trust Case Control Consortium; Genetic Investigation of ANthropometric Traits Consortium (2009). Six new loci associated with body mass index highlight a neuronal influence on body weight regulation. Nat. Genet. *41*, 25–34.

Zaltsman, Y., Shachnai, L., Yivgi-Ohana, N., Schwarz, M., Maryanovich, M., Houtkooper, R.H., Vaz, F.M., De Leonardis, F., Fiermonte, G., Palmieri, F., et al. (2010). MTCH2/MIMP is a major facilitator of tBID recruitment to mitochondria. Nat. Cell Biol. *12*, 553–562.